Slip Observer for Walking on a Low Friction Floor

Kenji KANEKO, Fumio KANEHIRO, Shuuji KAJITA, Mitsuharu MORISAWA
Kiyoshi FUJIWARA, Kensuke HARADA, *and* Hirohisa HIRUKAWA

National Institute of Advanced Industrial Science and Technology (AIST)
Tsukuba Central 2, 1-1-1 Umezono, Tsukuba, Ibaraki 305-8568, Japan

E-mail: {k.kaneko, f-kanehiro, s.kajita, m.morisawa, k-fujiwara, kensuke.harada, hiro.hirukawa}@aist.go.jp

Abstract

This paper presents a slip observer towards stabilizing biped walks on a low friction floor. Although biped humanoid robots are expected to easily adapt to environments designed for human, in fact they tend to tip over easily on real environments. For a practical use, it is one of important issues to stabilize a biped walking on an unexpected slippery floor with a low friction. In this paper, we propose the slip observer detecting skids that would occur at walking on unexpected slippery floor. We also propose a basic study of slip stabilizer towards reducing posture rolling caused by skids. Finally, we present experimental results using a humanoid robot HRP-2 to verify the validity of the proposed control scheme.

1. Introduction

Research on biped humanoid robots is currently one of the most exciting topics in the field of robotics. It is no exaggeration to say that the great success of HONDA humanoid robot makes the current research on the world's humanoid robot to become very active area [1-3]. Since the second prototype HONDA humanoid robot: P2 was revealed in 1996, many biped humanoid robots have been developed [4-11].

Biped humanoid robots are expected to easily adapt to environments designed for human, as they will be able to have better mobility than conventional wheeled robots. However, they tend to tip over easily on real environments in fact, even if stable walking patterns [12-16] that satisfy zero moment point (ZMP) stability criterion are carefully planned and biped humanoid robots faithfully replay them. The reason is that real environments are not consistent with supposed environments. During a biped walk on real environments, an actual ZMP of biped humanoid robots goes out of a desired ZMP planned by walking pattern generator. An error between the desired ZMP and the actual ZMP influences a stable biped walk and has a possibility to make biped humanoid robots tip over in the worst case. For a practical use of biped humanoid robots, it is important to stabilize a biped walking on real environments including unexpected conditions such as irregular terrains and unexpected slippery floor with a low friction.
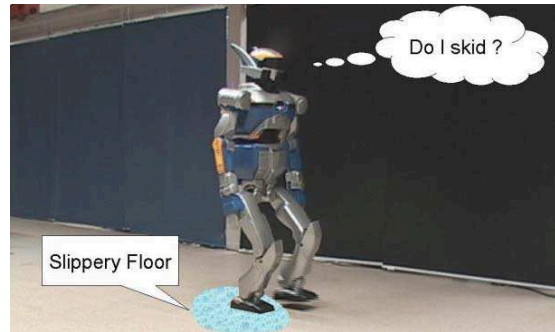

Figure 1. Walking on a slippery floor with a low friction

Several researches that focus on balance control have been studied recently. Hirose et al. proposed the walk stabilization based on ground reaction force control, desired ZMP control, and foot landing position control [3]. By using the walk stabilization, HONDA has achieved their biped humanoid robots with a posture stabilizing control similar to a human. Huang et al. developed a balance control combining dynamic walking patterns with real-time modification. In his papers, simulations [17] and experiments [10] showed that a robot was able to maintain stable walking and adapt to unknown environments by his balance controller. Kagami et al. presented an online algorithm for automatically generating dynamically stable compensations for humanoid robots [18]. This algorithm named "AutoBalancer," and modified the original input trajectories based on many criteria of stability. By experimental implementation into 16-DOF and 30-DOF humanoid robots, the effectiveness of "AutoBalancer" was demonstrated in his paper. The balance controller proposed by Sugihara and Nakamura also slightly modified a pre-designed motion trajectory, and that was achieved by manipulating the center of gravity (COG) with the whole-body cooperation using the COG Jacobian [19]. This balancing method was verified in some simulations using a model of existent biped humanoid robot. In the control system proposed by Löffler et al. [9], the trajectories of the ankle joint are modified depending on the orientation of the upper body and the torques between the foot and the ground. This control architecture is similar to an impedance control. Kim and Oh presented a balance control based on damping controller at ankle joint [11]. Their

experiments using real biped humanoid robots showed the effectiveness of their own balance controllers.

Although these balance controllers are going to increase stability of biped humanoid robots on the real environments, these controllers are not enough for a practical use because of no taking account of slippery floor. For example, biped robots for outdoor use should keep walking even if a sudden shower changes the condition between the foot and the ground. Manhole covers with rainwater would be slippery. It is one of important issues to stabilize a biped walking on an unexpected slippery floor with a low friction for a practical use.

In this paper, we considered an advanced balance control that enables the biped humanoid robots to adapt for sudden slips. To realize such balance control, we proposed the slip observer detecting skids that would occur at walking on unexpected slippery floor. We also proposed a basic study of slip stabilizer towards reducing posture rolling caused by skids. Finally, we presented experimental results using a humanoid robot HRP-2 [20] to verify the validity of the proposed control scheme.

2. Relevant Works

A few works that treated a biped locomotion on slippery environment have been studied so far.

Boone and Hodgins simulated a hopping robot on a floor with low friction area [21]. Their control method successfully overcame slipping and tripping by applying the reflex control. However, it is hard issue to apply their control method to a biped robot with foot soles.

Park and Kwon proposed a reflex control of biped robot locomotion on a slippery surface [22]. In this control, the hip link of the biped robot is lifted up vertically to increase the contact force between the foot and the ground at slipping. The desired acceleration of hip link in the vertical direction is calculated using the slipping velocity of the foot. However, this control is not suited for a practical use. One of reasons is that this control could run out of the elevation space of the hip link, as Park commented that by himself in his paper [22]. The second reason is that a deceleration of hip link is surely necessary after the hip link is once accelerated. Namely, the contact force between the foot and the ground would be surely decreased by deceleration of hip link. As a result, there is a possibility that the skid will get worse at that time. Another reason is that it is not easy to detect the velocity of the slipping foot in the real biped robot, while that information is easy calculated in the simulations.

Kajita et al. [23] proposed a method to generate walking patterns that take care of a low friction floor. The basic idea is based on reducing the friction between the foot and the ground, which is necessary at walking. To realize its idea, a preview control is utilized at generating the walking patterns. However, slips occur, if the real friction is smaller than the friction used in the pattern generator. Even if we use this pattern generation, it is requested for controller to have a function of real-time modification for an unexpected slippery floor.

3. Balance Control System of HRP-2

3.1. Overview of Control System

Figure 2 shows a balance control system employed in HRP-2. This control system consists of "Pattern Generator," "Joint Servo," "Kalman Filter," and "Stabilizer."

Our "Pattern Generator" shown in top-left of Figure 2 dynamically provides a stable walking pattern for HRP-2 and that is constructed using 3D linear inverted pendulum model and the preview controller [13, 14]. Output signals from this pattern generator are reference of joint angles and reference of ZMP. This desired reference of ZMP is described on the body base coordinate that is set up at between both crotch joints as shown in Figure 3.

"Joint Servo" shown in top-middle of Figure 2 faithfully replays a command of joint angles by feedback of joint angles. Here, the command of joint angles is made from modifying the reference of joint angles that is generated by "Pattern Generator" according to compensation signals of "Stabilizer." The sampling rate of "Joint Servo" is 1.0 [msec] on ART-Linux [24] that enables the execution of real-time processes at user level.
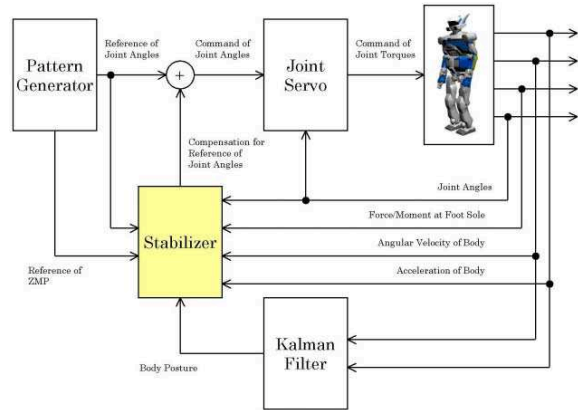

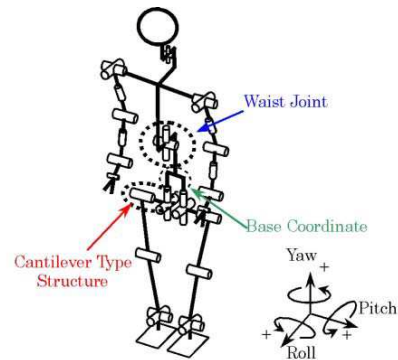Figure 2. Balance control system of HRP-2

Figure 3. Configuration of HRP-2

"Kalman Filter" shown in bottom-middle of Figure 2 calculates a posture of HRP-2's body, using 3-axes angular velocity sensor and 3-axes acceleration sensor. Compared to a complementary filter that calculates the body posture by acceleration signals with low-pass filter and integrated gyroscope signals with high-pass filter [9], "Kalman Filter" provides the trustworthy body posture. This calculated body posture, which consists of a roll-axis orientation, a pitch-axis orientation, and a yaw-axis orientation, is utilized in our "Stabilizer."

"Stabilizer" shown in center of Figure 2 calculates compensation signals from almost of all information used in the balance control system of HRP-2. Namely, the input signals to "Stabilizer" are output signals from "Pattern Generator," output signal from "Kalman Filter," and sensor signals such as joint angles, force/torque in the foot and in the wrist, acceleration of body, and angular velocity of body. The compensation signals calculated by "Stabilizer" are utilized for modifying the reference of joint angles generated by "Pattern Generator" to stabilize HRP-2's motions, such as pre-generated walking motions and pre-generated whole-body motions.

3.2. Overview of Stabilizing System

Figure 4 shows a stabilizing system employed in the balance control system of HRP-2. This stabilizing system consists of several sub-stabilizers, such as "Posture Stabilizer," "Rough Terrain Stabilizer," "ZMP Stabilizer," "Slip Stabilizer," and et al. Each output signal obtained by sub-stabilizer is added together as the final output signal of "Stabilizer." The principal sub-stabilizers are explained briefly in the following.

"Posture Stabilizer" shown in the top of Figure 4 plays a part in compensating posture rolling cause by mechanical compliance elements that are employed at the foot for absorbing landing shock [25]. The posture rolling that occurs during walking and working is also quickly recovered by using this sub-stabilizer.

"Rough Terrain Stabilizer" shown in the second block of Figure 4 plays a part in adapting to uneven surface. Due to this sub-stabilizer, HRP-2 was able to cope with uneven surface that we defined to have a height difference of less than 4 [cm] with inclines up to 5 [%], which are about 2.86 [deg.].
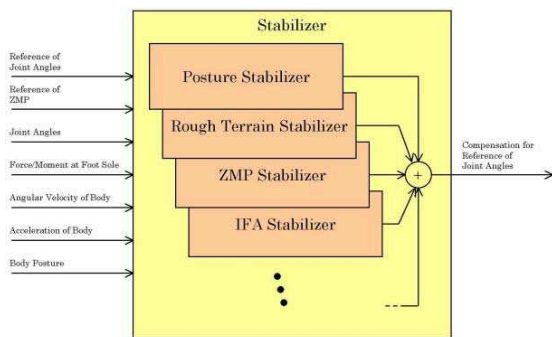

Figure 4. Stabilizing system of HRP-2

"ZMP Stabilizer" shown in the third block of Figure 4 plays a part in compensating posture rolling caused by errors between the desired ZMP and the actual ZMP. Owing to this sub-stabilizer, the ability in grounding feet was increased as if the foot sole was absorbing the ground.

"Slip Stabilizer" shown in the fourth block of Figure 4 plays a part in compensating posture rolling caused by skids between the foot and the ground. An algorithm of this sub-stabilizer is based on "Slip Observer" that detects skids. The proposed slip observer is explained in the next section.

4. Slip Observer

In this section, an advanced balance control that enables the biped humanoid robots to adapt for sudden slips is explained. To introduce the balance control for slip, the desired reaction force for walking is explained in connection with pattern generation in Section 4.1. We consider the reason why the biped humanoid robot slips and we define the slip force in Section 4.2. After introducing the slip observer that detects defined skids in Section 4.3, we consider how to suppress posture rolling caused by slips in Section 4.4.

4.1. Desired reaction force

The biped humanoid robots are not fixed on the ground, while the typical industrial manipulators are fixed. In order for the biped humanoid robots to walk on the floor, they need reaction forces from the floor. For example, the biped humanoid robots should kick the ground to walk. The reaction against kicking the ground accelerates and decelerates the body of biped humanoid robot.

Now, let us consider the desired reaction force. The solutions of reaction force for walking exist boundlessly. In the case of human, one of solutions would be reflexively selected, though the selected one is not always best. However, we defined here the desired reaction force for walking to be the selected one. In the case of biped humanoid robots, the desired reaction force is defined as the reaction against kicking that robots are going to replay according to the pattern generation.
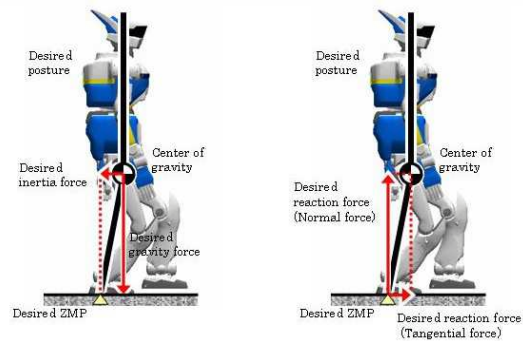
(a) Reference of ZMP   (b) Desired reaction force
Figure 5. Humanoid in the pattern generator's world

Namely, the desired reaction force of biped humanoid robot is given as the desired inertia force that is calculated at the pattern generation (see Figure 5). When we want to use the desired reaction force in the balance control, it is the best way to ask that to the pattern generator. If the pattern generator does not directly provide that for the balance control system, we should estimate that by using output signals from the pattern generator. In the balance control system of HRP-2 shown in Figure 2, since the pattern generator does not provide that, the desired reaction force is estimated as follows.

Our "Pattern Generator" is constructed using 3D linear inverted pendulum model. Under proper condition, a walking dynamics can be approximated by

$$p_x = x - (z_c / g) (d^2 x / dt^2) , \qquad (1)$$
$$p_y = y - (z_c / g) (d^2 y / dt^2) , \qquad (2)$$

where the x-axis is specified as the ordinal walking direction, (x, y) represents the horizontal displacement of the whole robot's center of mass (CoM), z_c is the height of the CoM, g is gravity acceleration, and (p_x, p_y) is the ZMP.

From Equations (1) and (2), the desired inertia force can be written as

$$M (d^2 x / dt^2) = - (p_x - x) M (g / z_c) , \qquad (3)$$
$$M (d^2 y / dt^2) = - (p_y - y) M (g / z_c) , \qquad (4)$$

where M is the total mass of the robot. As a result, the desired reaction force that is necessary for acceleration/deceleration of the robot body is obtained as the following equations.

$$f_x^{ref} = - (p_x - x) M (g / z_c) \qquad (5)$$
$$f_y^{ref} = - (p_y - y) M (g / z_c) \qquad (6)$$

Here, (f_x^{ref}, f_y^{ref}) is the desired reaction force. ($p_x - x$) and ($p_y - y$) indicate relative position from the CoM to the ZMP.

Considering that the CoM is nearly placed around the origin of the body base coordinate in the case of HRP-2's walking, an approximation of the desired reaction force can be written as

$$f_x^{ref} \approx - {}^b p_x^{ref} M (g / z_c) , \qquad (7)$$
$$f_y^{ref} \approx - {}^b p_y^{ref} M (g / z_c) , \qquad (8)$$

where (${}^b p_x^{ref}$, ${}^b p_y^{ref}$) represents relative position from the origin of the body base coordinate to the desired ZMP. Since our "Pattern Generator" provides (${}^b p_x^{ref}$, ${}^b p_y^{ref}$) for the balance control system as the desired reference of ZMP described on the body base coordinate, we have a possibility to estimate the desired reaction force using Equations (7) and (8).

However, the approximation of the desired reaction force obtained from Equations (7) and (8) is not suitable for a practical use. The reason is that an error between the CoM and the origin of the body base coordinate makes a steady-state error at the estimation of the desired reaction force. To remove this steady-state error, we can fortunately use the high-pass filter, since horizontal elements of the desired reaction force at standing are zero. We confirmed that the high-pass filtered approximation of the desired reaction force is almost the same as the truth of that. In the practical balance control system of HRP-2, Equations (9) and (10) are utilized to estimate the desired reaction force.

$$f_x^{ref} \approx - \text{HPF } {}^b p_x^{ref} M (g / z_c) \qquad (9)$$
$$f_y^{ref} \approx - \text{HPF } {}^b p_y^{ref} M (g / z_c) \qquad (10)$$

Here, HFP is a high-pass filter.

The schematic diagram of the estimation on desired reaction force is shown in Figure 6.

Figure 6. Estimation of desired reaction force

4.2. Definition of slip force

In this section, we consider a slip phenomenon and we define a slip force as a force leading to its slip phenomenon.

It is needless to say that the biped humanoid robot can behave as expected, if the actual reaction force is equal to the desired reaction force. If the biped humanoid robot can't receive an enough reaction force in spite of acting the ground, the slips between the foot and the ground occur.

In this paper, we regard this phenomenon as a slip phenomenon. Further, we consider the reason why the actual reaction force is not consistent with the desired reaction force is that the disturbance force acts on the foot from the ground. We define this disturbance force as a slip force. From this definition, the actual reaction force can be represented using the desired reaction force and the slip force as follows.

$$f_x = f_x^{ref} + f_{slip_x} \qquad (11)$$
$$f_y = f_y^{ref} + f_{slip_y} \qquad (12)$$

Here, (f_x, f_y) is the actual reaction force and (f_{slip_x}, f_{slip_y}) is the slip force.

In this paper, the slip force therefore can be defined by

$$f_{slip_x} \equiv - f_x^{ref} + f_x , \qquad (13)$$
$$f_{slip_y} \equiv - f_y^{ref} + f_y . \qquad (14)$$

4.3. Slip observer

Equations (13) and (14) tell us that we have a possibility to observe the slip force casing slip phenomenon.

The first term of right-hand side in Equations (13) and (14) is the desired reaction force. Using the pattern generator, this desired reaction force can be given or calculated as explained in Section 4.1.

The second term of right-hand side in Equations (13) and (14) is the actual reaction force. This actual reaction force can be obtained using a force/torque sensor embedded in the foot.

As a result, the slip force defined by Equations (13) and (14) can be observed by using both output signal of pattern generator and output signal of force/torque sensor embedded in the foot. Figure 7 shows the propose slip observer whose algorithm is given by Equations (13) and (14).
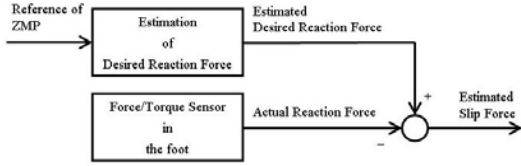

Figure 7. Slip observer

4.4. Stabilizing posture rolling

The slip has a possibility to make the biped humanoid robot tip over [23]. Even though the slipping biped humanoid robot does not tip over, the posture of body would not be little influenced by slip, that is to say, the posture rolling would not little occur at slipping. In this section we consider the control scheme to stabilize posture rolling caused by slips.

Now, let us consider a factor in posture rolling at slipping. As explained in Section 4.2, the slip force can be regarded as one of disturbance forces that act on the foot from the ground (see Figure 8(a)). With the consequence that the slip force acts the foot from the ground, the moment occurs around the CoM (see Figure 8(b)). This moment caused by slips is called the slip moment in this paper. As shown in Figure 8, this slip moment can be represented by

$$\tau_{slip_x} = + f_{slip_y} z_c , \qquad (15)$$
$$\tau_{slip_y} = - f_{slip_x} z_c , \qquad (16)$$

where (τ_{slip_x} , τ_{slip_y}) is the slip moment.

From the above discussion, it can be considered that this slip moment is the factor in posture rolling at slipping. By adjusting each foot's desired position and orientation according to this slip moment, the posture rolling at slipping is therefore suppressed in our slip stabilizer.
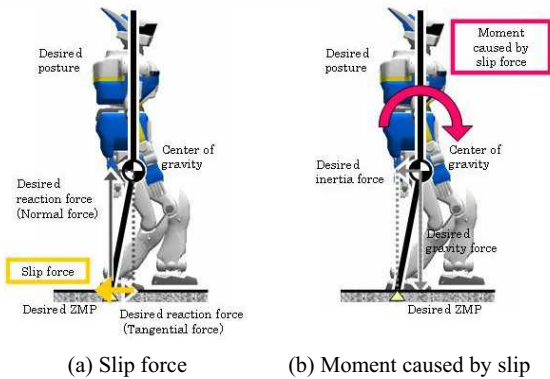

(a) Slip force   (b) Moment caused by slip
Figure 8. Humanoid in the real world at slipping

5. Experiments

To verify the validity of the proposed control scheme, we carried out experiments about walking on a low friction floor using a humanoid robot HRP-2 [20].

5.1. Imitating a low friction floor

The soles of HRP2 are covered by a rubber-like material, which offer the friction coefficient $\mu > 1.0$ on the lab floor. Since the friction coefficient $\mu > 1.0$ is out of the question for experiments about walking on a low friction floor, we set up a low friction floor condition. To obtain low-μ condition for entire walking, we attached plastic sheets on both soles of HRP-2. By putting HRP-2 on a steel floor coated by paint as shown in Figure 9, we were able to imitate a low friction floor. With the consequence that we measured the friction coefficient of imitated condition by directly pushing HRP-2 as shown in Figure 10, we obtained very low friction of $\mu = 0.144$ (see Table 1). This condition is practically the same as that of trodden and slippery snow for reference [26].
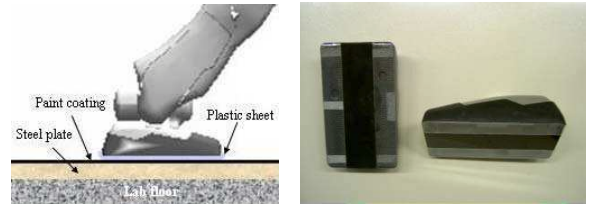
(a) Paint coating floor   (b) Foot sole with plastic sheets
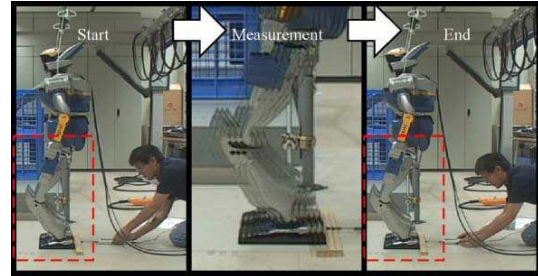Figure 9. Setup for imitating low friction floor

Figure 10. Measurement experiments on low friction floor

Table 1. Specification on friction coefficient

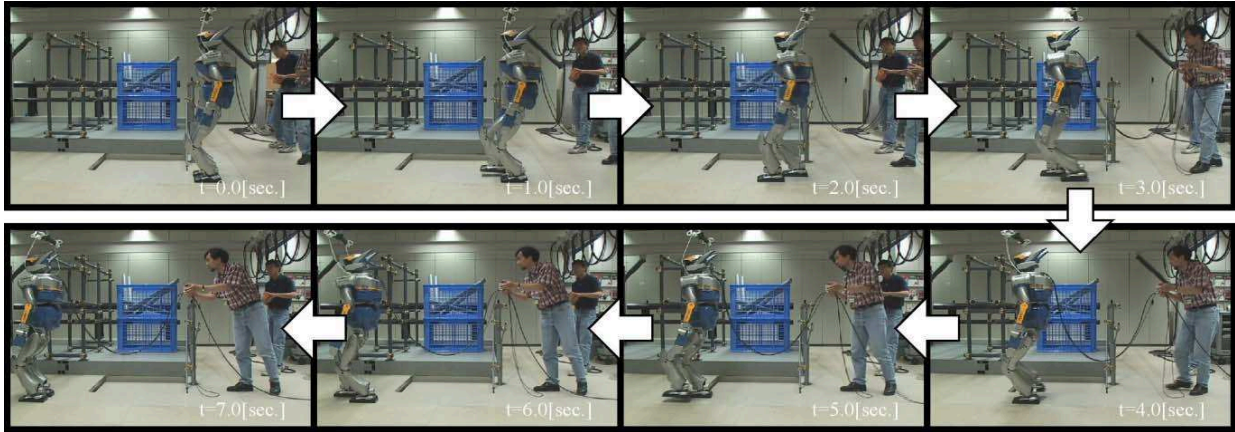|	Maximum of Pushing force	Contact force	Friction coefficient
1st trial	8.56 [kgf]		0.145
2nd trial	8.71 [kgf]		0.148
3rd trial	8.14 [kgf]		0.138
4th trial	8.58 [kgf]		0.145
5th trial	8.34 [kgf]	Robot weight:	0.141
6th trial	8.73 [kgf]	59.00 [kgf]	0.148
7th trial	8.50 [kgf]		0.144
8th trial	8.79 [kgf]		0.149
9th trial	8.34 [kgf]		0.141
10th trial	8.41 [kgf]		0.143
Average	8.51 [kgf]	59.00 [kgf]	0.144

Figure 11. Walk of 1.35 [km/h] on slippery floor whose friction coefficient is 0.14 (Sequence photographs: 1.0 [sec/frame])
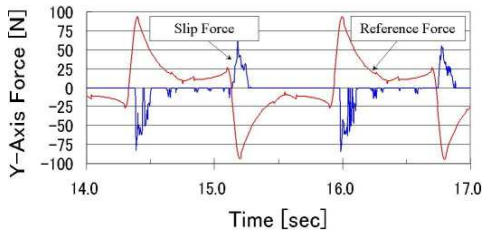

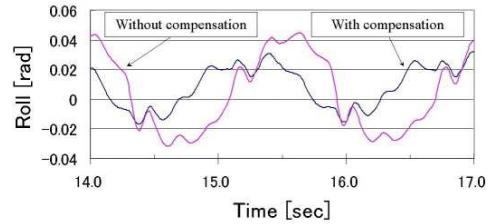Figure 12. Experimental results on slip observer

Figure 13. Basic experimental results on slip stabilizer

5.2. Walk on a floor μ=0.144

We tested a walk of 1.35 [km/h] on a low friction floor using a humanoid robot HRP-2. The used walking pattern was one prepared for normal lab floor, not for low friction floor. As explained in Section 5.1, the friction coefficient used in the experiments was μ = 0.144 which is practically the same as that of trodden and slippery snow. Against we expected, HRP-2 was successfully able to walk on a low friction floor with μ = 0.144 irrespective whether we employed the slip observer based compensation. However, it might be convenient for verifying the effectiveness of the slip observer based compensation. The reason is that the proposed control scheme based on slip observer suppresses the posture rolling caused by slips, not suppresses slip itself.

Figure 11 shows the experimental results on HRP-2's walk with the slip observer based compensation on a low friction floor. Eight photographs were taken sequentially every 1.0 [sec]. From Figure 11, we confirmed that HRP-2 was able to walk at 1.35 [km/h] on low friction floor with μ = 0.144.

Figures 12 and 13 show the experimental results indicating effectiveness of the proposed control scheme based on slip observer. The slip force obtained by proposed slip observer during walk on low friction floor and the roll-axis posture angle are shown in Figure 12 and Figure 13 respectively.

Figure 12 tells us that our propose slip observer detected big slip forces at the time when each leg touched the ground in consequence of switch from swing leg to support leg, while we observed slips at the same time shown in Figure 12 on visual inspection. From the experiments shown in Figure 12, we verified the effectiveness of the proposed slip observer.

Looking at Figure 13, it is observed that a posture variation of roll axis is less than 0.044 [rad] (≈ 2.5 [deg.]) when HRP-2 not compensated by slip observer based stabilizer walks on a low friction floor with μ = 0.144. Incidentally, the posture variation of roll axis was less than 0.017 [rad] (≈ 1.0 [deg.]) at walking on the lab floor with μ > 1.0 [25]. It is confirmed that the posture of body is not little influenced by slip, even if the slipping biped humanoid robot does not tip over. In case of experiments shown in Figure 13, slips influence the posture rolling that is 2.5 times as large as the posture rolling of non-slips. Figure 13 also tells us that a posture variation of roll axis is less than 0.030 [rad] (≈ 1.7 [deg.]) when HRP-2 compensated by slip observer based stabilizer walks on a low friction floor with μ = 0.144. Comparing these experimental results, it is apparent that the posture rolling was suppressed by employing the proposed control scheme based on slip observer.

6. Conclusions

This paper proposed an advanced balance control that enables the biped humanoid robots to adapt for an unexpected slippery floor. To realize such balance control, we first considered a slip phenomenon and we defined a slip force that is case of its slip phenomenon. After defining the slip force, we

proposed the slip observer detecting skids that would occur at walking on unexpected slippery floor. To reduce posture rolling caused by slips, we also proposed a basic study of slip stabilizer. Finally, we tested a walk of 1.35 [km/h] on low friction floor with μ = 0.144 using walking pattern prepared for high friction floor to verify the validity of the proposed control scheme. This condition of friction floor with μ = 0.144 is practically the same as that of trodden and slippery snow for reference [26].

Future works include more walking experiments on a floor of ultra-low friction (ex. μ = 0.1 which is said to be the friction on ice). Another future work is experiments about wide stride walk on low friction floor. The analyses and experiments for improving performance of proposed slip observer based balance controller are also our future work.

Acknowledgments

References

[1] K. Hirai, "Current and Future Perspective of Honda Humanoid Robot," Proc. IEEE/RSJ Int. Conference on Intelligent Robots and Systems, pp. 500-508, 1997.

[2] K. Hirai, M. Hirose, Y. Haikawa, and T. Takenaka, "The Development of Honda Humanoid Robot," Proc. IEEE Int. Conference on Robotics and Automation, pp. 1321-1326, 1998.

[3] M. Hirose, Y. Haikawa, T. Takenaka, and K, Hirai, "Development of Humanoid Robot ASIMO," Proc. IEEE/RSJ Int. Conference on Intelligent Robots and Systems, Workshop2 (Oct. 29, 2001), 2001.

[4] K. Nishiwaki, T. Sugihara, S. Kagami, F. Kanehiro, M. Inaba, and H. Inoue, "Design and Development of Research Platform for Perception-Action Integration in Humanoid Robot: H6," Proc. IEEE/RSJ Int. Conference on Intelligent Robots and Systems, pp. 1559-1564, 2000.

[5] Y. Kuroki, T. Ishida, J. Yamaguchi, M. Fujita, and T. Doi, "A Small Biped Entertainment Robot," Proc. IEEE-RAS Int. Conference on Humanoid Robots, pp. 181-186, 2001

[6] Y. Kuroki, M. Fujita, T. Ishida, K. Nagasaka, and J. Yamaguchi, "A Small Biped Entertainment Robot Exploring Attractive Applications," Proc. IEEE Int. Conference on Robotics and Automation, pp. 471-476, 2003.

[7] K. Nagasaka, Y. Kuroki, S. Suzuki, Y. ITOH, and J. Yamaguchi, "Integrated Motion Control for Walking, Jumping and Running on a Small Bipedal Entertainment Robot," Proc. IEEE Int. Conference on Robotics and Automation, pp. 3189-3194, 2004.

[8] M. Gienger, K. Löffler, and F. Pfeiffer, "Towards the Design of Biped Jogging Robot," Proc. IEEE Int. Conference on Robotics and Automation, pp. 4140-4145, 2001.

[9] K. Löffler, M. Gienger, and F. Pfeiffer, "Sensor and Control Design of a Dynamically Stable Bipe Robot," Proc. IEEE Int. Conference on Robotics and Automation, pp. 484-490, 2003.

[10] G. Wang, Q. Huang, J. Geng, H. Deng, and K. Li, "Cooperation of Dynamic Patterns and Sensory Reflex for Humanoid Walking," Proc. IEEE Int. Conference on Robotics and Automation, pp. 2472-2477, 2003.

[11] J. H. Kim and J. H. Oh, "Walking Control of the Humanoid Platform KHR-1 based on Torque Feedback Control," Proc. IEEE Int. Conference on Robotics and Automation, pp. 623-628, 2004.

[12] S. A. Setiawan, S. H. Hyon, J. Yamaguchi, and A. Takanishi, "Physical interaction between human and a bipedal humanoid robot – realization of human-follow walking –," Proc. IEEE Int. Conference on Robotics and Automation, pp. 361-367, 1999.

[13] S. Kajita, O. Matsumoto, and M. Saigo, "Real-time 3D walking pattern generation for a biped robot with telescopic legs," Proc. IEEE Int. Conference on Robotics and Automation, pp. 2299-2308, 2001.

[14] S. Kajita, F. Kanehiro, K. Kaneko, K. Fujiwara, K. Harada, K. Yokoi, and H. Hirukawa, "Biped Walking Pattern Generation by using Preview Control of Zero-Moment Point," Proc. IEEE Int. Conference on Robotics and Automation, pp. 1620-1626, 2003.

[15] Q. Huang, K. Yokoi, S. Kajita, K. Kaneko, H. Arai, N. Koyachi, and K, Tanie, "Planning Walking Patterns for a Biped Robot," IEEE Trans. on Robotics and Automation, Vol. 17, No. 3, pp. 280-289, June 2001.

[16] S. Kagami, K. Nishiwaki, T. Kitagawa, T. Sugihara, M. Inaba, and H. Inoue, "A Fast Generation Method of a Dynamically Stable Humanoid Robot Trajectory with Enhanced ZMP Constraint," Proc. IEEE Int. Conference on Humanoids, 31.pdf, 2000.

[17] Q. Huang, K. Kaneko, K. Yokoi, S. Kajita, T. Kotoku, N. Koyachi, H. Arai, N. Imamura, K. Komoriya, and K, Tanie, "balance Control of a Biped Robot combining Off-line Pattern with Real-time Modification," Proc. IEEE Int. Conference on Robotics and Automation, pp. 3346-3352, 2000.

[18] S. Kagami, F. Kanehiro, Y. Tamiya, M. Inaba, and H. Inoue, "Autobalancer: an online dynamic balance compensation scheme for humanoid robots," Proc. 4th Int. Workshop on Algorithmic Foundations of Robotics, pp. 329-340, 2000.

[19] T. Sugihara and Y. Nakamura, "Whole-body cooperative balancing of humanoid robot using COG Jacobian," Proc. IEEE/RSJ Int. Conference on Intelligent Robots and Systems, pp. 2575-2580, 2002.

[20] K. Kaneko, F. Kanehiro, S. Kajita, H. Hirukawa, T. Kawasaki, M. Hirata, K. Akachi, and T. Isozumi, "Humanoid Robot HRP-2," Proc. IEEE Int. Conference on Robotics and Automation, pp. 1083-1090, 2004.

[21] G. N. Boone and J. K. Hodgins, "Slipping and Tripping Reflexes for Bipedal Robots," Autonomous Robots, Vol. 4, pp. 259-271, 1997.

[22] J. H. Park and O. Kwon, "Reflex Control of Biped Robot Locomotion on a Slippery Surface," Proc. IEEE Int. Conference on Robotics and Automation, pp. 4134-4139, 2001.

[23] S. Kajita, K. Kaneko, K. Harada, F. Kanehiro, K. Fujiwara, and H. Hirukawa, "Biped Walking on a Low Friction Floor," Proc. IEEE/RSJ Int. Conference on Intelligent Robots and Systems, pp. 3546-3552, 2004.

[24] Y. Ishiwata and T. Matsui, "Development of Linux which has Advanced Real-Time Processing Function," Proc. RSJ Annual Conf., pp. 355-356, 1998 (in Japanese).

[25] K. Kaneko, S. Kajita, F. Kanehiro, K. Yokoi, K. Fujiwara, H. Hirukawa, T. Kawasaki, M. Hirata, and T. Isozumi, "Design of Advanced Leg Module for Humanoid Robotics Project of METI," Proc. IEEE Int. Conference on Robotics and Automation, pp. 38-45, 2002.

[26] "Manual of Northern Road," Report by Independent Administrative Institution Civil Engineering Research Institute of Hokkaido, http://www2.ceri.go.jp/koutsuu/rkanri_m.htm, (in Japanese).